Environmental Fluid Mechanics
https://doi.org/10.1007/s10652-018-09658-6

ORIGINAL ARTICLE

View metadata, citation and similar papers at core.ac.uk
brought to you by CORE
provided by Repositorio

representation: application to river flood management

I. Echeverribar[1] · M. Morales-Hernández[2] · P. Brufau[1] · P. García-Navarro[1]

Received: 14 March 2018 / Accepted: 26 December 2018
© Springer Nature B.V. 2019

Abstract

River floods can be simulated with the 2D shallow water system of equations using finite volume methods, where the terrain is discretized in cells that form the computational mesh. Usually a proper treatment of wet/dry fronts is required. River levees can be modelled as part of the topography by means of sufficiently small cells of higher elevation than the rest of the bed level in locally refined meshes. This procedure is associated with a large computational time since the time step depends directly on the cell size. The alternative proposed in this work includes the levees as internal boundary conditions in the 2D numerical scheme. In particular, levees have been defined by a weir law that, depending on the relative values of water surface levels on both sides, can formulate the discharge for different situations (i.e. free flow and submerged flow). In addition, having identified numerical difficulties in cases of low discharge under free flow conditions, a novel procedure to avoid oscillations has been developed and called volume transport method. The validation and comparison between methods has been carried out with benchmark test cases and, in addition, with a real flood event in the Ebro River (Spain)

Keywords Internal boundary condition · Finite volume · River flooding · Levees · Numerical modelling

✉ I. Echeverribar
echeverribar@unizar.es

M. Morales-Hernández
mmorales@unizar.es

P. Brufau
brufau@unizar.es

P. García-Navarro
pigar@unizar.es

[1] Fluid Mechanics, LIFTEC-EINA, CSIC-University of Zaragoza, Zaragoza, Spain

[2] Department of Soil and Water, EEAD-CSIC, Zaragoza, Spain

Published online: 07 January 2019

1 Introduction

River flood management has become an important tool since mankind settled in floodplains. In order to avoid the inundation of urban areas and to minimize the damage on cultivated lands and farms established near the rivers, hydraulic structures and control elements are placed on both sides along the river to protect them [4] by limiting the flood extension. Computational modelling is a useful tool to know the flow behaviour in general and, in particular, in presence of hydraulic structures, such as levees. [7, 11, 13].

Two-dimensional depth averaged models are quite suitable when dealing with flood events. The use of 2D models provides complete information about water depth and 2D plain velocity fields. However, the accuracy of the numerical results is very sensitive to the computational mesh used to discretize the terrain. Taking into account that the bed irregularities and structures, such as levees, govern the flow movement, the mesh cells shape and size have a significant influence on their correct representation [3] and may lead to different numerical results [14].

This work is focused on the modelling of levees in the context of a Finite Volume method. One possibility is based on sub-meshing techniques or local mesh refinement in order to reproduce them accurately. However, this leads to small time steps and high computational times due to the limiting cell size. Alternatively, in order to avoid the use of fine meshes or small time steps, levees can be modelled as *weirs* through *internal boundary conditions* (IBC), as sketched in Fig. 1. Depending on the relative values of the weir crest and the water surface levels on both sides, the IBC can represent different situations such as no flow crossing the levee or, in case of weir overtopping, free flow and submerged flow. In cases of small discharge free flow conditions, numerical difficulties have been identified and a novel procedure has been developed and called volume transport method (VTM).

This work is devoted to present different forms to model levees comparing both aforementioned approaches. The interest will be focused on their relative performance paying attention to both the quality of the numerical results (accuracy, oscillations and mass conservation) and the computational requirements (data storage and computational time). Results with and without the use of this method are presented to show the difference.

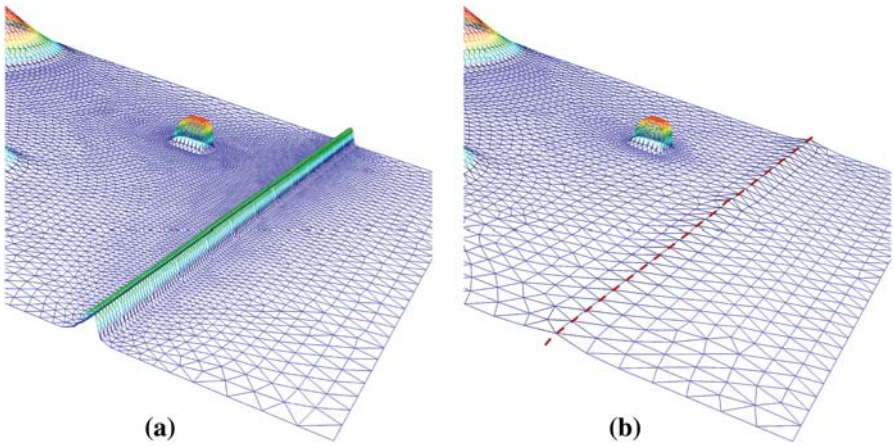

Fig. 1 Mesh used with a levee in terms of topography (**a**) and as internal boundary condition (**b**)

2 Governing equations and numerical scheme

2.1 2D shallow water equations

Flow evolution in rivers and floodplains can be described by means of depth averaged mass and momentum conservation equations:

$$\frac{\partial \mathbf{U}}{\partial t} + \frac{\partial \mathbf{F}(\mathbf{U})}{\partial x} + \frac{\partial \mathbf{G}(\mathbf{U})}{\partial y} = \mathbf{S}(\mathbf{U}) \tag{1}$$

with

$$\mathbf{U} = \begin{pmatrix} h \\ hu \\ hv \end{pmatrix}, \qquad \mathbf{F} = \begin{pmatrix} hu \\ hu^2 + g\dfrac{h^2}{2} \\ huv \end{pmatrix}, \qquad \mathbf{G} = \begin{pmatrix} hv \\ huv \\ hv^2 + g\dfrac{h^2}{2} \end{pmatrix},$$
$$\mathbf{S} = \begin{pmatrix} 0 \\ gh\left(S_{0x} - S_{fx}\right) \\ gh\left(S_{0y} - S_{fy}\right) \end{pmatrix} \tag{2}$$

where h, hu, hv are the conserved variables: water depth, unit discharge on x direction and unit discharge on y direction, respectively; $g = 9.81\ \mathrm{m/s^2}$ is the acceleration of gravity. The bed slopes, represent the spatial evolution of the bed level, z_b:

$$S_{0x} = -\frac{\partial z_b}{\partial x} \qquad S_{0y} = -\frac{\partial z_b}{\partial y} \tag{3}$$

and the friction slopes are defined in terms of the Manning roughness coefficient, n [1, 2, 6], as:

$$S_{fx} = \frac{n^2 u\sqrt{u^2+v^2}}{h^{4/3}} \qquad S_{fy} = \frac{n^2 v\sqrt{u^2+v^2}}{h^{4/3}} \tag{4}$$

2.2 Finite volume numerical scheme

System (1) has no analytical solution. A numerical scheme, defined on a computational mesh, is required in order to solve the problem. In this work, a first order upwind explicit finite volume numerical method is used and the system of Eq. (1) is integrated at each cell, acting like a control volume Ω limited by its contour C:

$$\frac{d}{dt}\int_{\Omega} \mathbf{U} d\Omega + \oint_{C} (\mathbf{E}\cdot\mathbf{n}) dl = \int_{\Omega} \mathbf{S} d\Omega \tag{5}$$

where $(\mathbf{E}\cdot\mathbf{n})$ represents fluxes in normal direction to C. Through the Jacobian matrix of these fluxes, the eigenvalues, $\tilde{\lambda}^m$, and eigenvectors, $\tilde{\mathbf{e}}$, are obtained and used to update each cell variables, as detailed in [9] and [12]. Finally, the expression at each cell of the mesh, i, is as follows [12]:

$$\mathbf{U}_i^{n+1} = \mathbf{U}_i^n - \frac{\Delta t}{A_i}\sum_{k=1}^{3}\sum_{m=1}^{3}\left[(\tilde{\lambda}^{-}\tilde{\gamma}\tilde{\mathbf{e}})_k^m l_k\right]^n \tag{6}$$

where A_i is the cell area, l_k represents the cell edge length and $\tilde{\gamma}_k$ stands for a compact representation of fluxes and source terms at each cell edge, k. Note the minus superscript denoting the ingoing contributions that arrive to each cell, following the upwind methodology. Finally, Δt is the time step, which is not constant during the simulation, but dynamically calculated as follows:

$$\Delta t = \mathrm{CFL} \min_{k,m} \frac{\delta x_k}{\tilde{\lambda}_k^m} \tag{7}$$

where

$$\delta x_k = \min(\chi_i, \chi_j) \qquad \chi_i = \frac{A_i}{\max_{k=1,NE} l_k} \tag{8}$$

and the CFL is the dimensionless parameter controlling stability under the criterion $0 < \mathrm{CFL} \leq 1$ for explicit numerical methods [8]. The numerical method is formulated to ensure well-balanced solutions in steady state and good behaviour in presence of wet/dry fronts avoiding always negative water depth and ensuring water volume conservation to machine precision.

2.3 Boundary conditions treatment

Equation (6) represents the variables updating scheme at each interior cell of the domain with the ingoing fluxes that come from the neighbour cells. This ingoing information is defined at cell edges thus, when dealing with triangular meshes, there are three fluxes to update the three conserved variables. However, boundary cells have a lack of information since at least one of their edges does not have a neighbour cell. Therefore, boundary conditions are needed to supply the missing information. In this work, these conditions are applied directly at the center of the boundary cell.

2.3.1 External boundary condition

The external boundary conditions set the inlet and outlet information regarding the flow conditions at the domain limits. In river simulation cases, a discharge hydrograph is the most common inlet boundary condition. In that case, the unit discharge is imposed at the center of the boundary cell following the normal direction to the inlet boundary edge whereas the water depth is provided by the numerical scheme (6). As outlet boundary condition, gauging curves $\mathrm{Q} = \mathrm{Q}(h + z_b)$ are widely used, as they introduce the information of the outlet cross sections, providing a relation between water depth and discharge. From the discharge updating provided by the numerical scheme (6), the external gauging law is used to evaluate the water level at the boundary cell.

2.3.2 Internal boundary condition

The presence of an internal hydraulic structure can be modelled by means of a mathematical condition imposed at an interior line within the computational domain. This is called internal boundary condition (IBC). Each pair of cells sharing an edge on that internal line are considered internal boundary cells. As in the case of the external boundary cells, these

cells are updated using both information from the numerical scheme and from the IBC. The particular formulation used is next presented.

3 Numerical modelling of the flow through a weir as an IBC

In a 2D model representing levees as part of the topography, those cells are solved as ordinary cells using (6). However, when dealing with IBC, a special method is required for their treatment. Figure 1 illustrates the two alternatives. In particular, Fig. 1b shows a coarse mesh around an embankment that is used in combination with an internal boundary line (highlighted in red) used to characterize the levee crest mathematically. Figure 2a shows an example of IBC defined along an internal boundary line. Several pairs of cells (filled with blue in Fig. 2a) lie on both sides of the line sharing an edge. Since they are not introduced in the normal computing procedure, an external law is used to define the module of the discharge through them while the water depth is provided by the numerical scheme (6). It is worth stressing that the discharge is assumed normal to the direction of the shared edge. This procedure ensures volume conservation but introduces directionality in the flow. This could be considered a limitation and it will be evaluated with a test case in later sections.

Assuming the flow direction from left to right as in Fig. 2a the upstream element is called cell 1 and the downstream is cell 2. The whole procedure assumes, without loss of generality, that $d_1 > d_2$, being $d = h + z_b$ the free surface level (see Fig. 2b). The assumption of $d_2 > d_1$ is analogous.

Water surface elevation levels, provided by the numerical scheme (6), are used to evaluate the discharge through the levee by means of an external discharge expression. The flow computation is governed by $H = d - h_{z,weir}$, i.e., the difference between the water depth and the weir crest, that can be defined on both sides of the weir (see Fig. 2b). Therefore, several cases must be taken into consideration:

1. If $h_{z,weir} > max(d_1, d_2) \rightarrow H_1^n < 0$, the normal flow is null and the weir behaves as a solid wall.

$$q_1^{n+1} = q_2^{n+1} = q = 0 \tag{9}$$

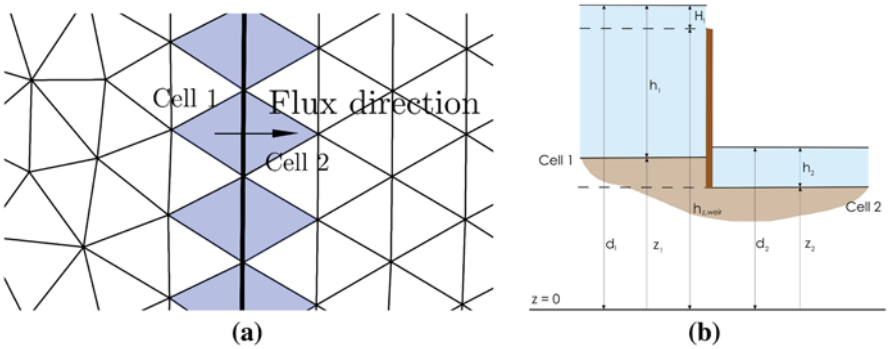

Fig. 2 Diagram of flux through a weir in a 2D triangular mesh. Plane view (**a**) and lateral view (**b**)

2. If $(d_1, d_2) > h_{z,weir} \rightarrow H_1^n, H_2^n > 0$, a discharge is computed through the weir following [6, 15]

$$q_1^{n+1} = q_2^{n+1} = q = C_d \frac{2}{3}\sqrt{2g}(H_1^n)^{3/2}\left(1 - \left(\frac{H_2^n}{H_1^n}\right)^{3/2}\right)^{0.385} \tag{10}$$

where C_d is a energy loss coefficient which needs to be calibrated. In this work the value used is C_d=0.611 [6].

3. If only $d_1 > h_{z,weir} \rightarrow H_1^n > 0$, the same discharge law with $H_2 = 0$ [Eq. (11) (free flow)] is used to compute the flow through the weir [6].

$$q_1^{n+1} = q_2^{n+1} = q = C_d \frac{2}{3}\sqrt{2g}\left(H_1^n\right)^{3/2} \tag{11}$$

with the same value for C_d coefficient as used in (10). In this case, attention must be paid not only to the discharge, but also to the downstream water depth. The procedure differs depending on h_2^n and $h_{cr} = h_{cr}(q, h_2)$, that is the critical depth associated to q.

(a) If $h_2^n > h_{cr}$, only the discharge is imposed and h_2^{n+1} is provided by the numerical scheme

(b) If $h_2^n \leq h_{cr}$ a special treatment is required. Here, the volume transport method (VTM) is proposed. The critical depth is imposed downstream and this represents a volume addition to that cell. That same volume is withdrawn from the upstream cell in order to ensure mass conservation. That additional volume is:

$$V = \left[h_{cr} - h_2^n\right]A_2 \tag{12}$$

leading to,

$$h_2^{n+1} = h_{cr}. \tag{13}$$

And it implies an updating on upstream cell:

$$h_1^{n+1}A_1 = h_1^n A_1 - V \tag{14}$$

It is worth noting that the help of a tolerance ξ is required to avoid oscillations when deciding the sign of H_1, since the removed volume from upstream cell could lead to negative values of H_1^n. Therefore, H_1^n must be enough to ensure critical depth as follows:

$$\begin{aligned} &h_2^n + \frac{H_1^n A_1}{A_2} \geq h_{cr} \\ &H_1^n \geq \frac{\left(h_{cr} - h_2^n\right)A_2}{A_1} = \xi \\ &H_1^n \geq \xi \end{aligned} \tag{15}$$

It is worth stressing that the described levee modelling approach, VTM, is proposed to avoid model instabilities in cases where a levee cell fills to the limit where the water levels upgradient (d_1) and the levee crest ($h_{z,weir}$) are similar and the downstream cell has a low or nil water depth. This could happen at the early stage of levee overtopping.

4 Results

Several theoretical and practical benchmark cases are presented next in order to test the method under different conditions. First, a test case with a frontal impact of the flood wave against a levee is presented to illustrate the application of the VTM approach. A second test case focuses on the momentum alteration associated to the proposed formulation of the IBC. Finally, the method is applied to rivers and real cases.

4.1 Frontal test case

This case is defined to show the sensitivity of the results to the different choices in the levee representation and formulation. In particular, to demonstrate the necessity of the VTM condition. It is a case restricted to purely normal flow to the levee.

4.1.1 Test case description

Figure 3 shows the terrain elevation of the test case, z_b (m), with two different color maps: a scale which encompasses the whole height range (a); and an upper bounded scale to display the terrain irregularity and the micro-topography (b). The test case contains an embankment, several obstacles and ten probes that have been distributed upstream and downstream the hydraulic structure (yellow points in Fig. 3a).

Four approaches have been set to represent the levee and to compare their suitability. They are illustrated in Fig. 4, where a detail of the 2D mesh can be seen on the left together with a sketch of the associated terrain elevation representation on the right (the actual terrain profile is represented in black, the mesh cells in blue and the IBC is depicted in red). The four strategies are described below:

- Strategy R (Reference): the whole domain is finely meshed. It is displayed in Fig. 4a. The levee crest is properly captured by means of small cells as well as the floodplain.
- Strategy A (locally refined): the levee is captured with a fine mesh as in case R, but the floodplain is represented with a coarser mesh, as seen in Fig. 4b.
- Strategy B (IBC with modified mesh): the whole domain is meshed with large cells and the levee crest is not well captured. However, an internal boundary condition (IBC) is used to characterize the levee (see Fig. 4c). In addition, the bed level at the upstream and downstream cells is manually reduced in order to represent the levee only in IBC terms.

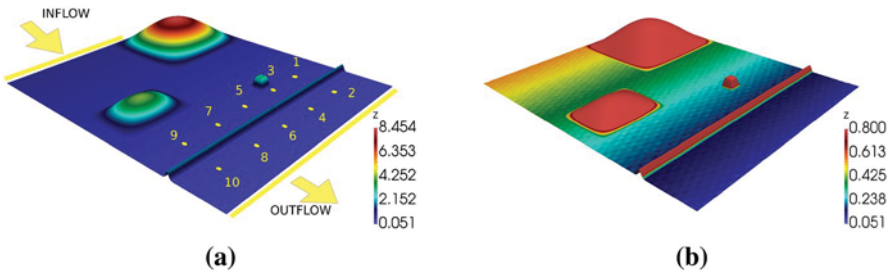

Fig. 3 3D view of the test case analysed (**a**) and detail of micro topography (**b**)

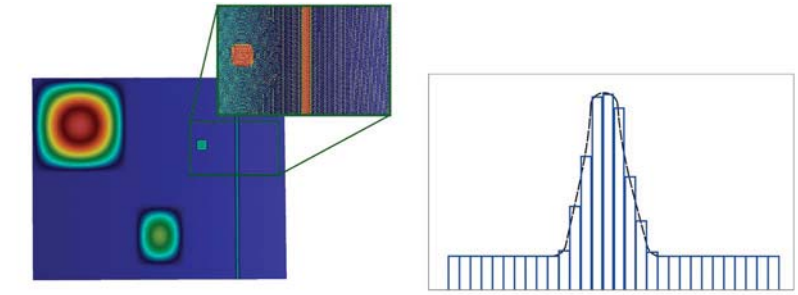

(a) Strategy R

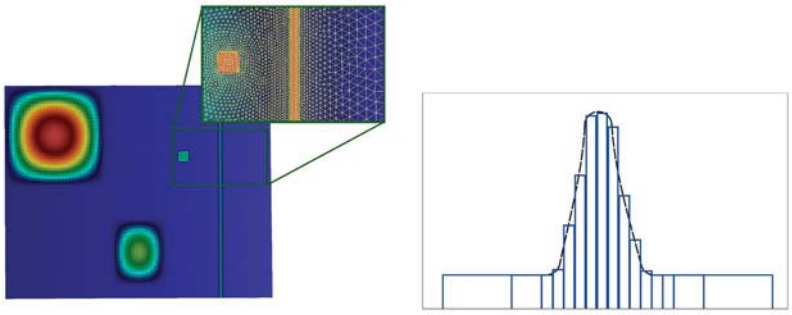

(b) Strategy A

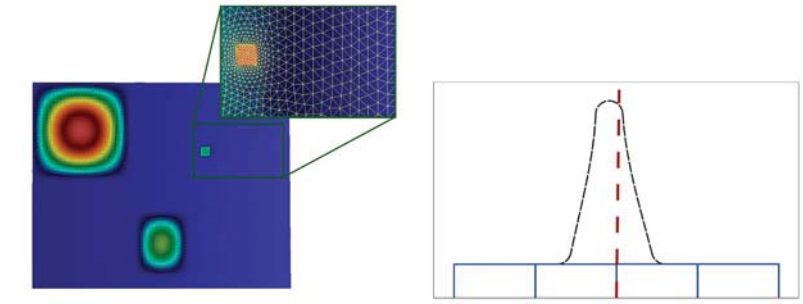

(c) Strategy B

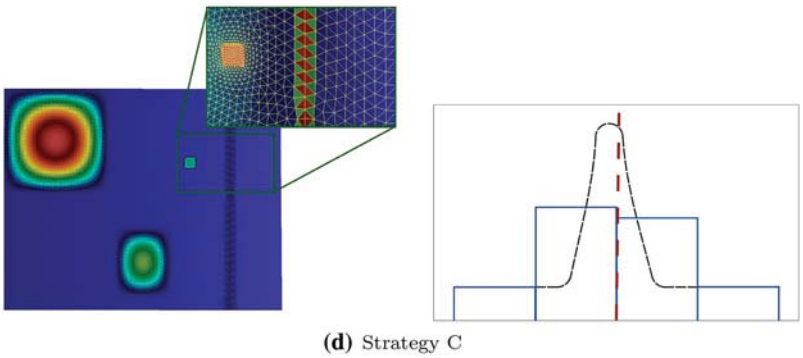

(d) Strategy C

Fig. 4 Detail of the mesh for each representation approach (left) and numerical discrete representation of the levee topography (right)

- Strategy C (IBC without mesh modification): similar to the method followed in case B, but without the manual decrease on upstream and downstream cells. Therefore, this case represents the hydraulic structure crest in terms of IBC, however some cells are elevated due to the mesh generation procedure and the original terrain elevation (see Fig. 4d).

The difference between approaches B and C is the modification of the bed level elevation at some cells along the IBC line (blue cells in Fig. 2a), since the use of IBC is supposed to substitute the characterizations by means of cell elevation. In case C, when meshing the original data, the elevation of IBC cells is unavoidably affected by the embankment and thus, the hydraulic structure would be represented twice (by means of topography and by means of IBC). On the other hand, case B has been modified not to have elevated cells and to represent the levee only by means of a discharge law.

The external boundary conditions can be seen in Fig. 3a. A constant discharge of 1 m^3/s is set as inlet boundary condition and a gauging curve is used as outlet BC. Flow enters over a dry terrain as initial condition. The evolution of water surface elevation (WSE) at the probes has been compared for the four meshes and for different inlet discharges. Results can be seen in Fig. 5.

4.1.2 Test case results

Figure 5(left) shows the results in terms of WSE evolution at probes without the use of the tolerance in the VTM method. It is seen that when dealing with a low discharge such as 1 m^3/s, the IBC's strategies present oscillations at downstream cells due to the small quantity of water passing through the levee, governed by the volume transport method (VTM) and due to the fast wetting and drying transitions at the downstream cell.

After the use of the mentioned tolerance, the same simulations have been carried out and the results provided by the method are now shown in Fig. 5(right). The critical situations in which VTM was oscillating are overcome, and this method is improved to become a robust approach.

Assuming mesh R as a reference, both representations, A (with fine mesh), B and C (with IBC), provide quite accurate results. However, the number of cells in mesh A (14,138 cells) is higher than in meshes B and C (7066 cells), which leads to the reduction of the computational time when using the approach proposed here.

Regarding the use of IBC, several strategies can be adopted, since cells elevation will unavoidably represent levee presence (see Fig. 4d), though not properly due to the coarse mesh. In order to characterize the embankment only in terms of IBC, strategy B is adopted and cells are manually modified. However, this becomes highly tedious and C strategy is also carried out to test the influence of those elevated cells. After evaluating the results, the scarce elevation of these cells does not influence the results excessively, as seen in Fig. 5. It must be recalled that the WSE is the sum of the bed elevation and the water depth. Therefore, the WSE can be different at dry points in a domain with non-zero bed gradient. Therefore, it can be concluded that strategy B is not necessary when using IBC, since its results are quite similar to those from strategy C but harder to carry out.

Fig. 5 Temporal evolution of WSE(m) without the use of tolerances (left) and with the use of tolerances ▶ (right) at probes 3, 4, 5 and 6 for Q = 1 m^3/s

4.2 Lateral test case

With the aim of analysing the flow behaviour in the case of a lateral overflow, a terrain model that provides a flow tangential to a levee has been simulated. The test case is used to evaluate the influence of the levee model as an IBC on the velocity field.

4.2.1 Test case description

In this test a rectangular channel 800 m long and 200 m wide with a 0.005 longitudinal slope is assumed. A levee is located at the left margin high enough to avoid cross-flow except along a lower gap from x = 180 m to x = 600 m. A flat horizontal bed is assumed at the other side of the levee. Initial conditions are dry bed everywhere and a uniform roughness coefficient n = 0.04 is assumed. A constant discharge of 80 m^3/s is imposed as inlet BC at the channel inlet boundary and free outflow condition is set downstream.

4.2.2 Test case results

Figure 6 show the *y* velocity component distribution at four times (t = 200 s, t = 380 s, t = 800 s and t = 1500 s). The position of the levee is indicated with a dotted line. The figure contains three modelling alternatives: on the left Fig. 6a, d, g, j correspond to the results obtained on a very fine mesh representing the levee as ordinary cells by means of submeshing techniques. Figure 6b, e, h, k, have been obtained using the same fine mesh but including the levee represented with an IBC. Figure 6c, f, i, l display the results from the simulation on a x15 times coarser mesh with the levee also represented as an IBC. Figure 7 is the plot of the *x* velocity component in the same cases.

Figures 6 and 7, show that the flow enters the domain parallel to the levee (*y* direction) so that overflow takes place at t = 200 s [subfigures (a, b, c)]. From that time, the levee acts as a free flow weir. In the representation of the levee as an IBC the flow direction is forced to be transversal to the structure. However, the resulting velocity field is almost identical to that obtained when modelling the levee as topography. This can be seen in Figs. 6 and 7, where the represented times are: t = 200 h (a, b, c), t = 380 h (d, e, f), t = 800 h (g, h, i) and t = 1500 s (j, k, l).

The comparison between the different simulations reports very similar results. This is due to the fact that the free flow over the weir represented a topography tends to have a transversal direction to the structure, and the momentum in the *y* direction decreases significantly. The most relevant difference that may be observed appears between the two meshes used in combination with the IBC case (see center and right pictures in Figs. 6 and 7). It is worth stressing that the use of a coarser mesh always implies a reduction on the accuracy in the results, and the user must have this into consideration. However, this test shows that, with the same mesh, the use of an IBC or a sub-meshing technique does not lead to very different results. Therefore, the test case is useful to justify that, although the discharge is forced to be normal to the levee direction in the IBC model, this is a local effect and the velocity field is almost identical to the one computed with the other levee representation.

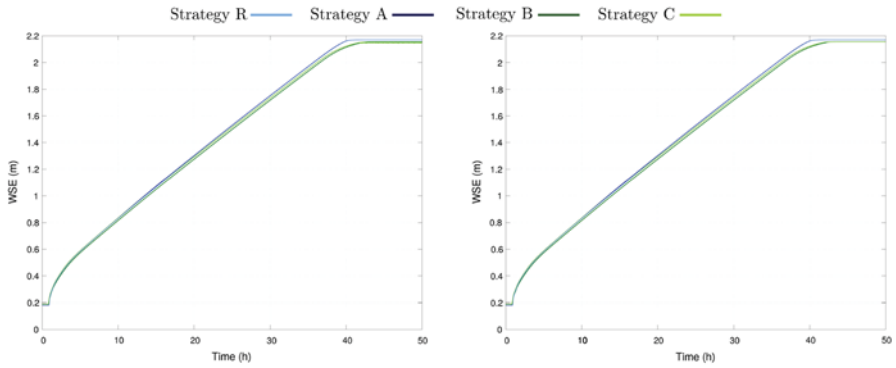

Probe 3

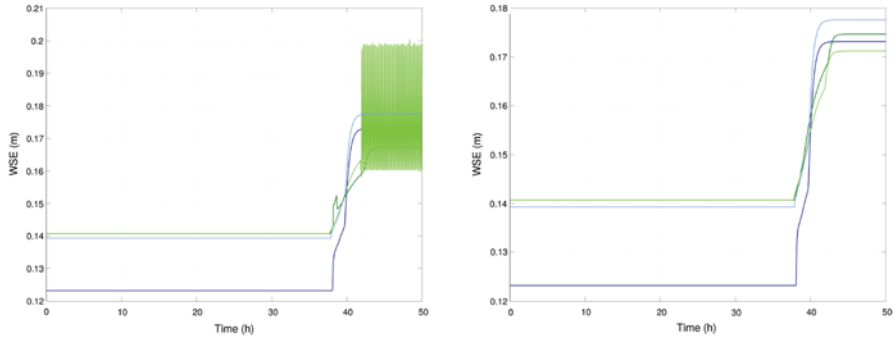

Probe 4

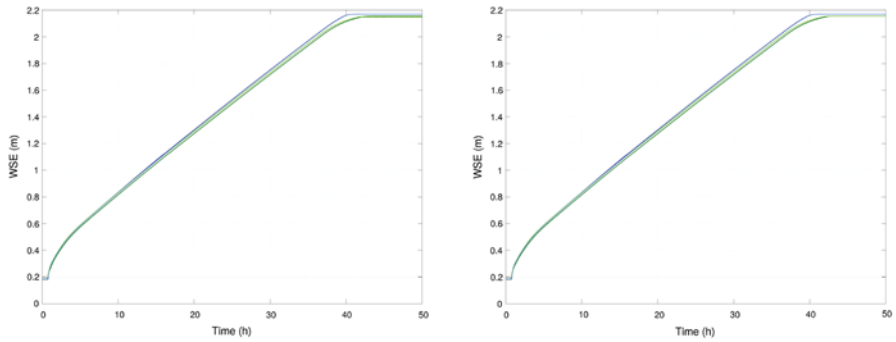

Probe 5

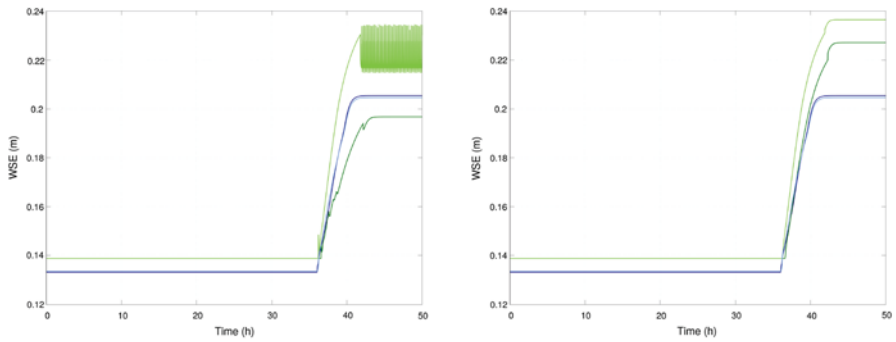

Probe 6

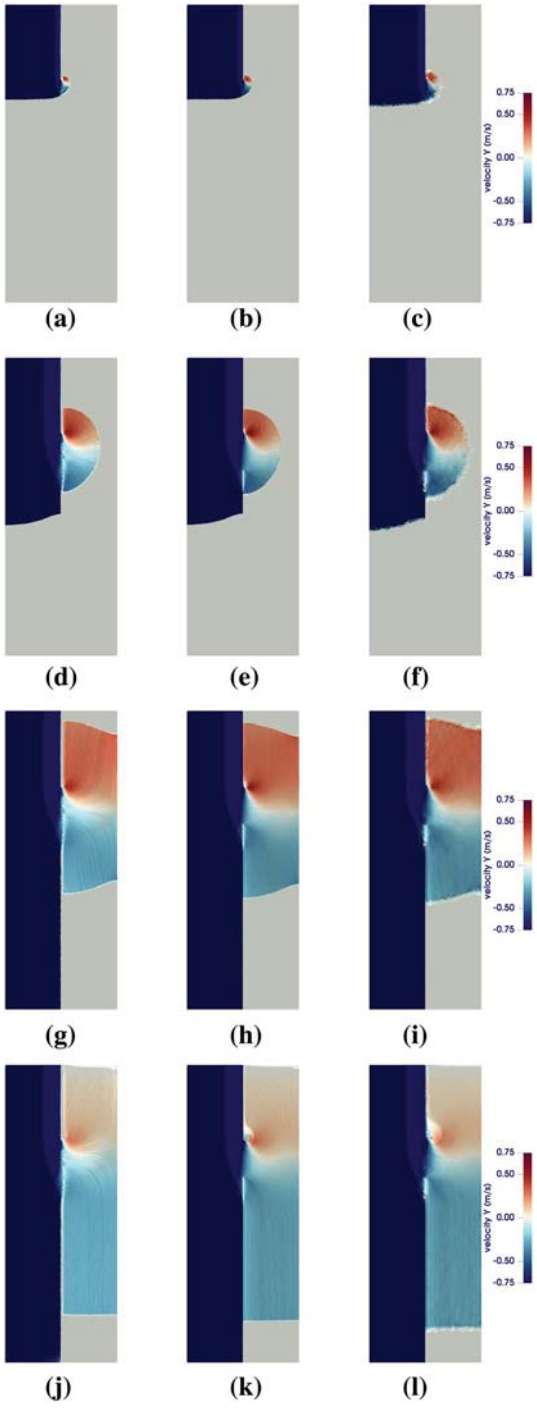

Fig. 6 Time evolution of y-velocity. **a**, **d**, **g**, **j** On a fine mesh with the levee represented as topography, **b**, **e**, **h**, **k** on a fine mesh with the levee represented with an IBC and **c**, **f**, **i**, **l** on a coarser mesh with the levee represented with an IBC

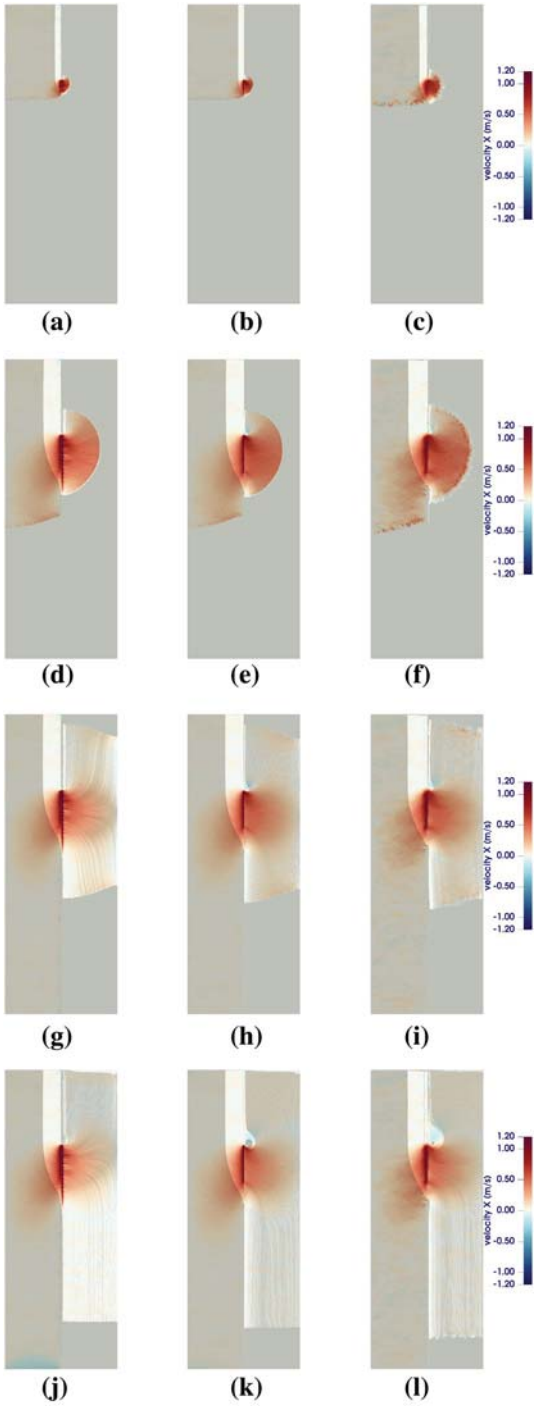

Fig. 7 Time evolution of x-velocity. **a**, **d**, **g**, **j** On a fine mesh with the levee represented as topography, **b**, **e**, **h**, **k** on a fine mesh with the levee represented with an IBC and **c**, **f**, **i**, **l** on a coarser mesh with the levee represented with an IBC

4.3 Application to the Severn River UK Benchmark test case

In order to apply the developed alternative to a realistic situation, the 7th benchmark test case included in [10] in the Severn River (United Kingdom) has been carried out. A small reach that encompasses 9 km of river bed has been simulated with a wave-shaped hydrograph as inlet boundary condition and a gauging curve as outlet boundary condition (see [10]). To model the levees present on the floodplain two strategies have been used: option A, using only topography representation with mesh refinement and Option C representing levees as IBC. This is illustrated in Fig. 4.

When representing the levees as part of the topography (Option A), a mesh with 85,775 cells is required. However, only 66,163 cells have been used for the terrain representation in Option C. This difference leads to a lower simulation time when computing the flood evolution, as seen in Table 1, where the computational time needed to simulate 72 h of real event (by means of an Intel CORE I7-4770 CPU parallelized 8 cores) is displayed.

Figure 8 illustrates the evolution of the simulated flooded area for both approaches: A (a, d, g) and C (b, e, h). On green scale the terrain elevation is represented, while the blue scale is for water depth. A detail of the representation of one of the levees is also presented in Fig. 8a, b in order to highlight the difference on cell size between the two strategies. In addition, a third column (c, f, i) contains the difference in flood depths, in order to easily show the similarity between inundation patterns.

In order to analyse the differences between the results provided by both strategies, some probes have been also defined. They are represented with blue dots in Fig. 8. Figure 9 shows the water surface elevation (WSE) time evolution comparing Option C with Option A. They are similar, presenting only a few discrepancies at the beginning of the simulation, when the floodplain is still dry and the terrain elevation discretization is not exactly the same due to the different cell size distribution on both meshes.

With the aim of obtaining a quantification of the pattern of coincidence between the two approaches, the flooded area is computed and compared following Eq. (16) [5] and results are shown in Table 2 for different moments of the simulation.

$$Fit_A(\%) = 100 \cdot \frac{A_1 \cap A_2}{A_1 \cup A_2} \tag{16}$$

where A_1 stands for the total wetted area of the simulation with the sub-meshing technique and A_2 corresponds to the IBC simulation. As it is seen in the Table, the results from both methods in terms of extension of the flooded area are quite similar.

4.4 Application to the Ebro River

In order to demonstrate a practical application of this technique, a real large-scale flood event of 21 days in a reach of the Ebro River (Spain), which contains 5 levees, has been run

Table 1 Simulation time for A and C meshes for Severn flood event

Mesh	N cells	Flood event duration (h)	Simulation time
A	85,775	72	15 h
C	66,163	72	12 h 26 min

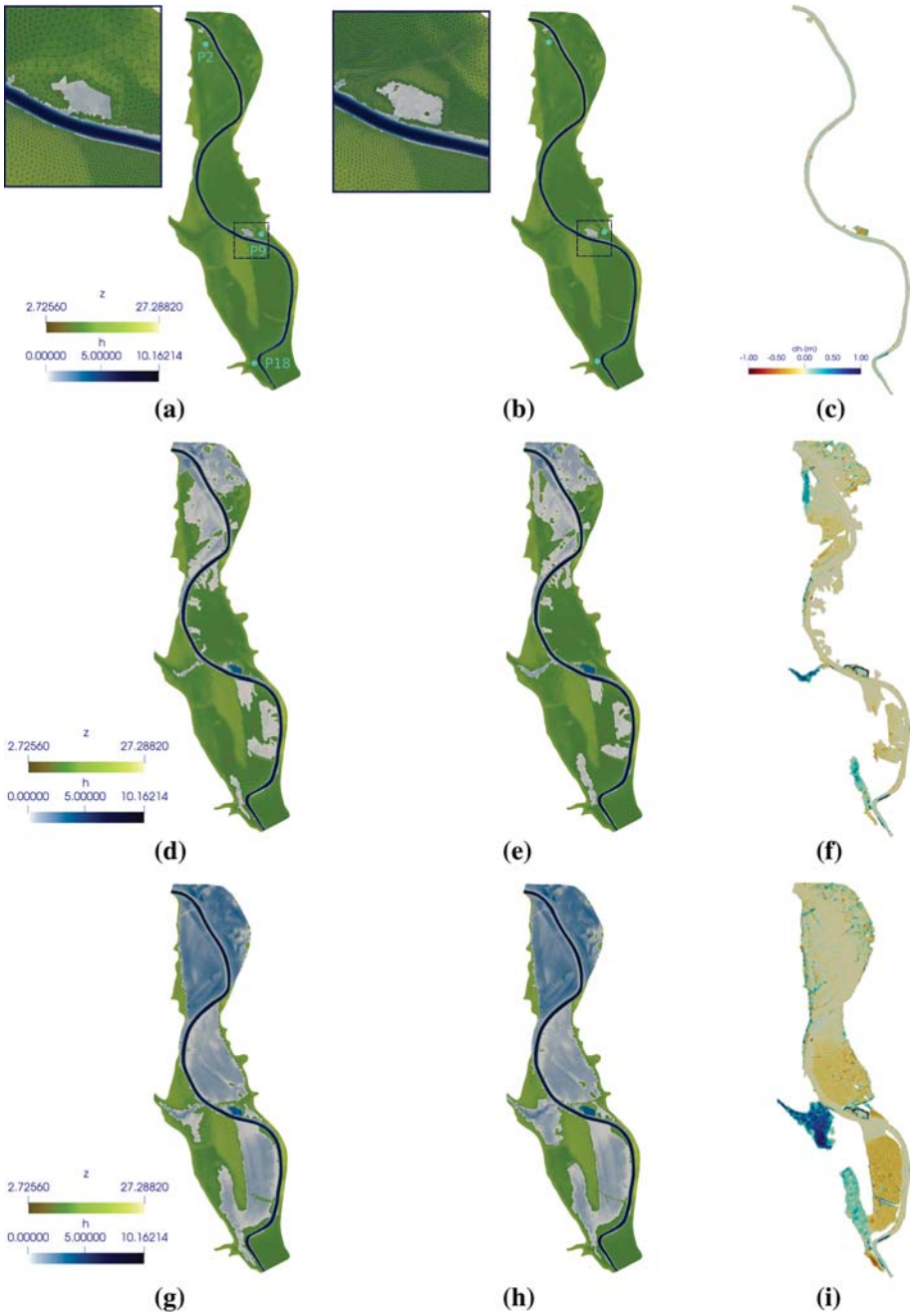

Fig. 8 Comparison of maximum flooded area between IBC use (**a**, **d**, **g**) and topography (**b**, **e**, **h**) and they water depth differences (**c**, **f**, **i**) at different times: t = 2 h (**a**–**c**), t = 4 h (**d**–**f**) and t = 8 h (**g**–**i**)

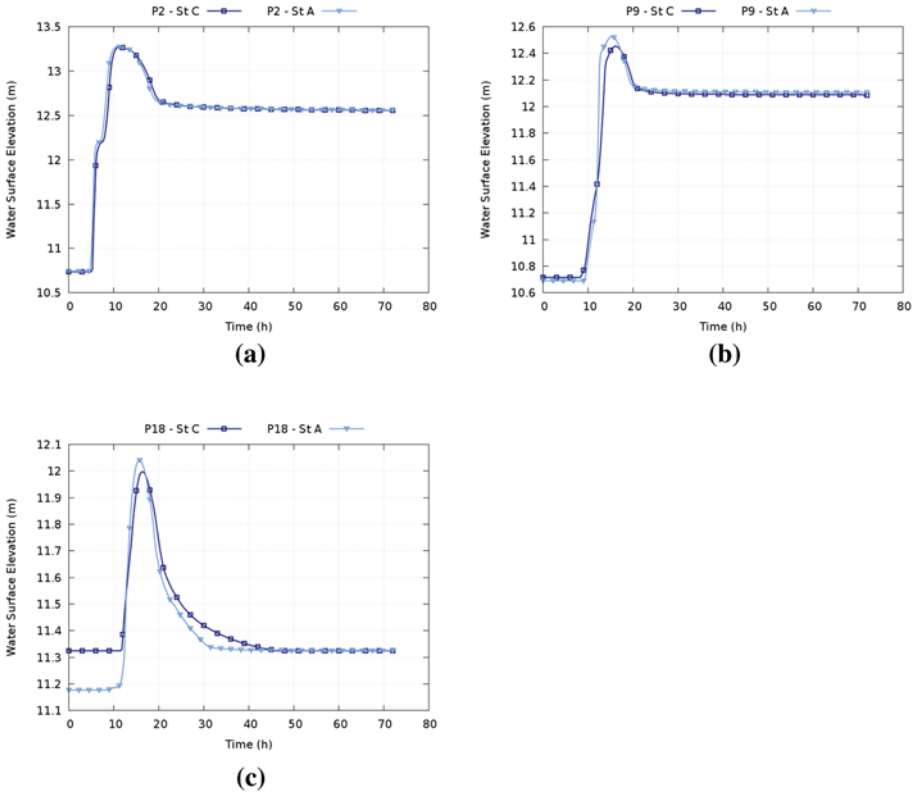

Fig. 9 Temporal evolution of WSE (m) at probes benchmark test case at Severn River comparing IBC (dark blue) with mesh refinement (light blue)

Table 2 Fit between strategies in terms of flooded area

	t = 2 h	t = 4 h	t = 8 h
Fit (%)	96.96	85.11	93.37

comparing both methodologies: strategy A (local mesh refinement technique) and strategy C (IBC without mesh modification).

The topography with the levees detail can be seen in Fig. 10a. The inlet BC is a hydrograph representing the flood event and a gauging curve is used as outlet BC.

Seven probes have been distributed along the computational domain, as seen in Fig. 10a. Probe 1 is the only located at the river bed, while the rest have been placed near the levees on the floodplain. Probes 3, 5 and 7 are not reached by water and remain dry up to the end of the simulation, therefore the evolution of the WSE is displayed only for the rest in Fig. 10b–d. As in the previous tests, there exists a discrepancy on the results at the beginning of the simulation for probes located at the initially dry floodplain. This is caused by the mesh elevation assignment associated to differences in cell size between both strategies.

Both simulations have been carried out on GPU (GeForce GTX Titan Black) to accelerate the calculations. The computational time values can be seen on Table 3. Strategy A,

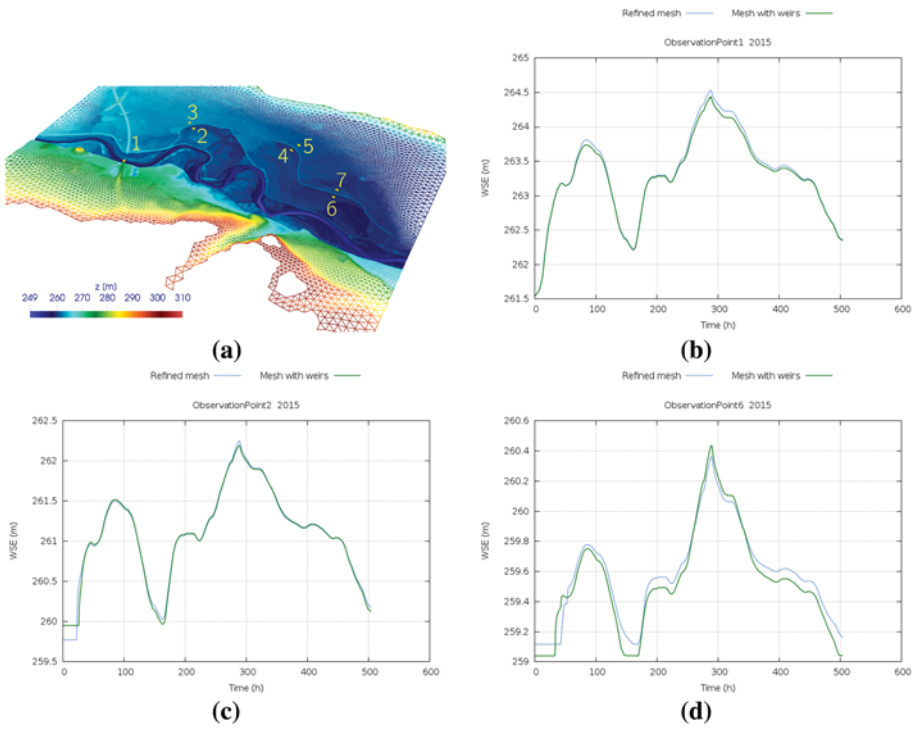

Fig. 10 Probes distribution (**a**) and temporal evolution of WSE (m) (**b**–**d**) in 2015 flood event case

Table 3 Simulation time for A and B meshes

Mesh	N cells	Flood event duration (days)	Simulation time
A	160,000	21	2 h 42 min
C	56,447	21	1 h 22 min

with the refined mesh used to characterize the levee, contains 160,000 cells whereas Strategy C uses a mesh with only 56,447. This leads to a reduction in computational time, not only due to the total number of cells, but also because smaller cells have been removed and they control the time step size (7).

5 Conclusions

Levees modelling is essential when dealing with flood event simulations, since they govern flow evolution, preventing areas to be flooded. Usually they involve a high computational cost due to the necessity of small cell sizes to represent them as part of the topography. This can be a problem when dealing with a great amount of these hydraulic structures in realistic cases. This work presents an alternative, modelling them as internal boundary conditions (IBC). With this approach, a special treatment is required and weir laws are used.

Two test cases have been carried out to compare the strategies throwing some conclusions: first, the use of IBC and, therefore, external weir laws requires a special treatment within the numerical scheme that allows the simulation of all flow regimes: no flow, free overflow and submerged overflow. The use of tolerances results crucial in extreme cases where free flow discharge is low to avoid oscillations in the numerical solution and a new algorithm has been provided.

On the other hand, as the IBC option offers the possibility to avoid local mesh refinement, this leads to a different terrain discretization that may produce different results. The difference found between the two different approaches that are related with IBC (B and C meshes) has resulted to be negligible, which is quite interesting for real cases where the process of manual mesh modification is unaffordable.

The IBC formulation proposed involves forcing the discharge direction normal to the levee. The consequences of this procedure on the global velocity field have been found to be negligible in the cases presented.

Two realistic simulations have been tested, the Severn inundation from the UK Benchmark Test Cases and a real Ebro River inundation event. In both cases the IBC formulation (C) and the topography representation (A) of the levees has been used. Although C has been applied to allow larger cells than A, the results obtained with both models are very similar in terms of time, extension of the flooded area and values of the variables.

Therefore, by the use of the proposed IBC, faster results have been obtained thanks to the possibility of using larger cell sizes instead of those used to finely follow the levee topography. On the other hand, a compromise can be found to avoid losing accuracy when using locally larger cells with this approach. This strategy has turned out to be a good alternative for these structures representation when domains involving a large number of cells are studied during long time periods and a mesh optimization becomes critical.

Acknowledgements This work was partially funded by the MINECO/FEDER under research Project CGL2015-66114-R and by Diputacion General de Aragon, DGA, through Fondo Europeo de Desarrollo Regional, FEDER. The third author also wants to thank to the MINECO for his Research Grant DI-14-06987.

References

1. Arcement GJ, Schneider VR (1984) Guide for selecting Manning's roughness coefficients for natural channels and flood plains, 2339 U.S. Geological Survey (Water Supply paper)
2. Chanson H (2004) Hydraulics of open channel flow. Butterworth-Heinemann, Oxford
3. Caviedes-Voullieme D, Garcia-Navarro P, Murillo J (2012) Influence of mesh structure on 2D full shallow water equations and SCS curve number simulation of rainfall/runoff events. J Hydrol 448:39–59
4. Di Baldassarre G, Casterllarin A, Brath A (2009) Anlaysis of the effects of levee heightening on flood propagation: example to the River Po, Italy. Hydrol Sci J 54(6):1007–1017
5. González-Sanchís M, Murillo J, Latorre B, Comín F, García-Navarro P (2012) Transient two-dimensional simulation of real flood events in a mediterranean floodplain. J Hydraul Eng ASCE 138(7):629–641
6. Henderson FM (1966) Open channel flow. Macmillan series in civil engineering. McGraw-Hill, New York
7. Jaffe DA, Sanders BF (2001) Engineered levee breaches for flood mitigation. J Hydraul Eng 127(6):471–479
8. Leveque R (2002) Finite volume methods for hyperbolic problem. Cambridge University Press, New York
9. Murillo J, García-Navarro P, Burguete J, Brufau P (2007) The influence of source terms on stability, accuracy and conservation in two-dimensional shallow flow simulation using triangular finite volumes. Int J Numer Methods Fluids 54(5):543–590

10. UK Environmental Agency (2010) Benchmarking of 2D hydraulic modelling packages, Environment Agency Report
11. Morales-Hernández M, Murillo J, García-Navarro P (2013) The formulation of internal boundary conditions in unsteady 2D shallow water flows: application to flood regulation. Water Resour Res 80:225–232
12. Morales-Hernández M, Hubbard ME, García-Navarro P (2014) A 2D extension of a large time step explicit scheme (CFL > 1) for unsteady problems with wet/dry boundaries. J Comput Phys 263:303–327
13. Remo JWF, Carlson M, Printer N (2012) Hydraulic and flood-loss modelling of levee, floodplain, and river management strategies, Middle Mississippi River USA. Nat Hazards 61:551–575
14. Schubert JE, Sanders BF, Smith MJ, Wright NG (2008) Unstructured mesh generation and landcover-based resistance for hydrodynamic modelling of urban flooding. Adv Water Resour 31:1603–1621
15. Villemonte JR (1947) Submerged-Weir discharge studies. Engineering News Record

Publisher's Note Springer Nature remains neutral with regard to jurisdictional claims in published maps and institutional affiliations.